

Operantly Conditioned Motoneuron Plasticity: Possible Role of Sodium Channels

JOHN A. HALTER, JONATHAN S. CARP, AND JONATHAN R. WOLPAW

Division of Restorative Neurology and Human Neurobiology, Baylor College of Medicine, Houston, Texas 77030; and Wadsworth Center for Laboratories and Research, New York State Department of Health and State University of New York, Albany, New York 12201-0509

SUMMARY AND CONCLUSIONS

1. Learning is traditionally thought to depend on synaptic plasticity. However, recent work shows that operantly conditioned decrease in the primate H reflex is associated with an increase in the depolarization needed to fire the spinal motoneuron (V_{DEP}) and a decrease in its conduction velocity (CV). Furthermore, the increase in V_{DEP} appears to be largely responsible for the H-reflex decrease. The conjunction of these changes in V_{DEP} and CV suggests that an alteration in Na^+ channel properties throughout the soma and axon could be responsible.

2. A mathematical model of the mammalian myelinated axon was used to test whether a positive shift in the voltage dependence of Na^+ channel activation, a decrease in Na^+ channel peak permeability, or changes in other fiber properties could have accounted for the experimental findings.

3. A positive shift of 2.2 mV in Na^+ channel activation reproduced the experimentally observed changes in V_{DEP} and CV, whereas a reduction in Na^+ channel permeability or changes in other fiber properties did not.

4. These results are consistent with the hypothesis that operantly conditioned decrease in the primate H reflex is largely due to a positive shift in the voltage dependence of Na^+ channel activation. Recent studies suggest that change in activation of protein kinase C may mediate this effect.

INTRODUCTION

Learning is thought to depend mainly on activity-driven changes in synaptic connections (Kandel 1991). Other potential sites, such as the soma and axon hillock, have received relatively little attention, although their properties can change with conditioning (e.g., Matsumura and Woody 1986). Recently, Carp and Wolpaw (1994) found that operantly conditioned decrease in the primate triceps surae H reflex, the electrical analogue of the monosynaptic spinal stretch reflex (Wolpaw and Herchenroder 1990), was accompanied by a 2.1-mV increase in the depolarization required to reach motoneuron firing threshold (V_{DEP}) and a 4.4-m/s decrease in axonal conduction velocity (CV).¹ No significant changes were noted in resting membrane potential or in other measured electrophysiological properties. The change in V_{DEP} , combined with a small decrease in the excitatory postsynaptic potential amplitude, appeared sufficient

to explain the change in behavior (i.e., a smaller H reflex). At present the mechanisms of the V_{DEP} increase and the CV decrease remain unknown.

Both these effects, and the accompanying absence of other effects, could be due to modification of Na^+ channels. Modification of Na^+ channels at the initial segment could affect threshold, whereas their modification at the nodes of Ranvier could affect axonal CV. Recent reports suggest two possible mechanisms: 1) positive shift in the voltage dependence of Na^+ channel activation (Dascal and Lotan 1991; Meiri and Gross 1989) and 2) reduction in Na^+ channel peak permeability (Gershon et al. 1992).

The present theoretical analysis tests these hypothesized mechanisms by using a recent model of the mammalian myelinated axon to predict the effects that each would have on CV, V_{DEP} , and action-potential amplitude (APA) and compares these predicted effects to the experimental observations of Carp and Wolpaw (1994). In addition, the uniqueness of these predictions is evaluated by assessing model behavior in response to modifications of parameters other than Na^+ channels. The results provide additional indication that the plasticity of nonsynaptic neuronal properties is a component of learning. Preliminary reports of this study have appeared in abstract form (Halter et al. 1993, 1994).

METHODS

This analysis uses a distributed-parameter model (Halter and Clark 1991) to simulate a mammalian myelinated nerve fiber that is 2 cm long, 17.5 μm diam, and contains 10 nodes of Ranvier. The model geometry (Table 1) is derived from an anatomic ultrastructural description by Berthold and Rydmark (1983), which includes detailed representation of the node of Ranvier, the paranodal myelin sheath attachment region, the noncylindrical fluted region, and the stereotyped internodal region. The myelin sheath is comprised of 165 lamellae (nl) with single lamella thickness (mt) of 0.0153 μm . With the use of an assumption of radial symmetry and employing a nonuniform spatial discretization, an electrical equivalent network is derived from this geometry. The axolemma is represented by an electrical circuit containing nonlinear conductances for the sodium and potassium (fast and slow-gated) channels, and linear conductances for the leakage channels.

In the model, axoplasmic and periaxonal resistivities (ρ^i and ρ^p) are 70 Ωcm , specific conductances for the nodal axon (G_{ax}), internodal axon (G_{ax}^*), and nodal gap (G_{ng}) are 156, 1, and 7×10^4 mS/cm², respectively, and the specific capacitance for the axon (C_{ax}) is 1 $\mu\text{F}/\text{cm}^2$. The effective specific capacitance (C_{my}) and conductance (G_{my}) of the myelin sheath are determined by

¹ Because CV differs for gastrocnemius and soleus motoneurons, average values for operantly conditioned gastrocnemius and soleus motoneurons were weighted according to their proportions in the naive (i.e., unconditioned) gastrocnemius and soleus populations before calculating this average decrease.

TABLE 1. Geometric parameters

Node of Ranvier	Length	1.5
	Radius	2.5
	Periaxonal space width (effective)	0.03
	Nodal gap length	0.27
Paranodal myelin sheath attachment region	Length	4
	Proximal Radius	2.2
	Distal Radius	2.4
	Periaxonal space width	0.001
	Myelin sheath thickness	2.5
Noncylindrical fluted region	Length	75
	Proximal radius (axial)	5.1
	Distal radius (axial)	6.25
	Proximal radius (radial)	9
	Distal radius (radial)	6.25
	Periaxonal space width	0.003
	Myelin sheath thickness	2.5
Internodal region	Length	1,800
	Radius	6.25
	Periaxonal space width	0.001
	Myelin sheath thickness	2.5

All dimensions are in micrometers. References to proximal and distal are relative to the node of Ranvier.

$$X_{my} = \{b \cdot \sum_{i=0}^{n-1} [x^{my} \cdot 2\pi(b + i \cdot mt + mt/2)]^{-1}\}^{-1}$$

where $x = C = 0.5 \mu\text{F}/\text{cm}^2$ for the capacitance and $x = G = 1 \text{ mS}/\text{cm}^2$ for the conductance and b is the radius of the inner lamella of the myelin sheath. Specific permeabilities (in $\text{cm s}^{-1} \times 10^{-3}$) are 74.1 Na, 0.078 Na*, 0.375 K_{fast}, 0.0624 K*_{fast}, 0.0937 K_{slow}, 0.0312 K*_{slow} (where * denotes internodal). In the resting state, membrane potential (E_r) is -78 mV , and leak current reversal potentials for the nodal (E_{leak}) and internodal E_{leak}^* regions are -77.9625 and -76.48 mV , respectively. Ion concentrations (in mM) are 154 [Na]_{out}, 8.71 [Na]_{in}, 5.9 [K]_{out}, and 155 [K]_{in}. The distributed-parameter model can be described as a system of two coupled partial differential equations

$$C_{ax} \frac{\partial V^i}{\partial t} = \frac{a}{2\rho^i} \frac{\partial^2 V^i}{\partial x^2} + C_{ax} \frac{\partial V^p}{\partial t} - J_{ax}$$

and

$$(aC_{ax} + bC_{my}) \frac{\partial V^p}{\partial t} = \frac{a^2 + b^2}{2\rho^p} \frac{\partial^2 V^p}{\partial x^2} + aC_{ax} \frac{\partial V^i}{\partial t} + aJ_{ax} - bJ_{my}$$

where V^i and V^p are the intra-axonal and periaxonal potentials relative to an external common reference potential; a is the axonal radius, and $b - a$ is the width of the periaxonal space; J_{ax} is the summation of the component axolemmal ionic current densities $J_{Na} = P_{Na} m^3 h x(\text{Na})$, $J_{Kf} = P_{Kf} n_f^4 x(\text{K})$, and $J_{Ks} = P_{Ks} n_s^4 x(\text{K})$, where $x(Z) = EF^2/RT/[Z]_o - [Z]_i \exp(EF/RT)/[1 - \exp(EF/RT)]$ for $Z = \text{Na}$ or K , $T = 310^\circ\text{K}$, $R = 8.31 \text{ J} \cdot (\text{mole} \cdot ^\circ\text{K})^{-1}$, $F = 96,478 \text{ C} \cdot \text{mole}^{-1}$ and $E = V^i - V^p$; and $J_{my} = G_{my} \cdot V^p$ for the myelin and $G_{ng} \cdot V^p$ for the nodal gap. The gating variables are described by the ordinary differential equation

$$dx/dt = (x_\infty - x)/\tau_x \quad \text{with} \quad x_\infty = \alpha_x/(\alpha_x + \beta_x) \quad \text{and}$$

$$\tau_x = 1/(\alpha_x + \beta_x) \quad \text{for} \quad x = m, h, n_f, n_s$$

where a separate representation for the α and β rate constants is used to compute the steady-state (x_∞) and time constant (τ_x) terms for n_f and n_s , and where (with $V = E - E_r$) α_m , α_{onf} , α_{rnf} , α_{ons} , $\alpha_{\text{rns}} = A(V - B)/\{1 - \exp[(B - V)/C]\}$; β_m , β_{onf} , β_{rnf} , β_{ons} , $\beta_{\text{rns}} = A(B - V)/\{1 - \exp[(V - B)/C]\}$; $\alpha_h = A(V + B)/\{\exp[(V + B)/C] - 1\}$; and $\beta_h = A/\{1 + \exp[(B - V)/C]\}$ with the use of the coefficients in Table 2. The Na⁺ channel-gating variables are described at $T = 293^\circ\text{K}$ and the K⁺ channels at $T = 289.5^\circ\text{K}$. Both were adjusted to $T = 310^\circ\text{K}$ with the use of the following Q_{10} temperature coefficients: α_m , β_m , 2.2; α_h , β_h , 2.9; α_{nf} , α_{ns} , 3.2; and β_{nf} , β_{ns} , 2.8. The model parameters were derived

from a compendium of myelinated nerve fiber properties formed from the literature (Halter 1989). A detailed development of the distributed-parameter model can be found in Halter and Clark (1991).

The coupled system of partial differential equations was numerically integrated with an implicit algorithm similar in form to the Crank-Nicolson method, with the use of 221 discrete spatial segments. One segment was used for each of the 10 nodes, 4 for each myelin sheath attachment region (80 total), 4 for each fluted region (80 total), 5 for each standard internodal region (45 total), and 3 for each of the 2 terminal internodal regions (6 total). Sealed end conditions were assumed, and a temporal step size of $0.1 \mu\text{s}$ was used. Simulations were performed with a Silicon Graphics Indigo R4400 computer.

CV was calculated from the arrival times of the action potential at the two central nodes of Ranvier. The parameter set defined above produced a CV of 71.4 m/s, matching that observed in triceps surae motoneurons of unconditioned animals. Changes in APA were determined from the axonal transmembrane potentials present at one of these nodes during simulation of saltatory conduction. V_{DEP} was determined by measuring the peak axonal transmembrane potential generated during application of a just-subthreshold current (i.e., rheobase minus 10 pA) to one of the central nodes of Ranvier (Fig. 1A). This provided a standardized measure of the peak axonal transmembrane potential in the highly nonlinear region of the firing threshold (Fig. 1B).

To assess our initial hypothesis that conditioning-induced alterations in motoneuron properties (Carp and Wolpaw 1994) resulted from changes in Na⁺ channel properties, the experimentally observed 4.4-m/s decrease in CV was reproduced in the model by changing 1) the voltage dependence of Na⁺ channel activation by altering the B activation rate constant coefficients, 2) the time constant of Na⁺ channel activation, 3) the voltage dependence of Na⁺ channel inactivation by altering the B inactivation rate constant coefficients, 4) the time constant of Na⁺ channel inactivation, or 5) the nodal Na⁺ channel peak permeability. To explore alternative possibilities (i.e., change in other active or passive properties or in fiber structure), the CV decrease was also mimicked by changing 6) peak permeability of nodal K_{fast} channels, 7) peak permeability of nodal K_{slow} channels, 8) nodal axonal conductance, 9) myelin capacitance, 10) number of myelin lamellae, 11) fiber diameter, or 12) paranodal periaxonal space width. Each parameter modification was uniform across the model fiber. For each of these 12 different parameter changes, the concurrent effects on V_{DEP} and APA were determined.

RESULTS

Modification of each of the 12 parameters changed CV. Figure 2A shows the predicted dependence of CV on Na⁺ channel activation voltage (—) and on Na⁺ channel peak

TABLE 2. Rate constant coefficients

	A, ms ⁻¹	B, mV	C, mV
α_m	0.49	25.41	6.06
β_m	1.04	21.00	9.41
α_h	0.09	27.74	9.06
β_h	3.70	56.00	12.50
α_{onf}	0.54	1.32	2.94
β_{onf}	1.51	35.06	7.82
α_{rnf}	0.0078	-20.17	38.85
β_{rnf}	0.0214	17.88	0.91
α_{ons}	3.83	-15.73	16.44
β_{ons}	2.11	45.56	18.85
α_{rns}	0.00092	-25.75	15.73
β_{rns}	0.0042	0.24	8.54

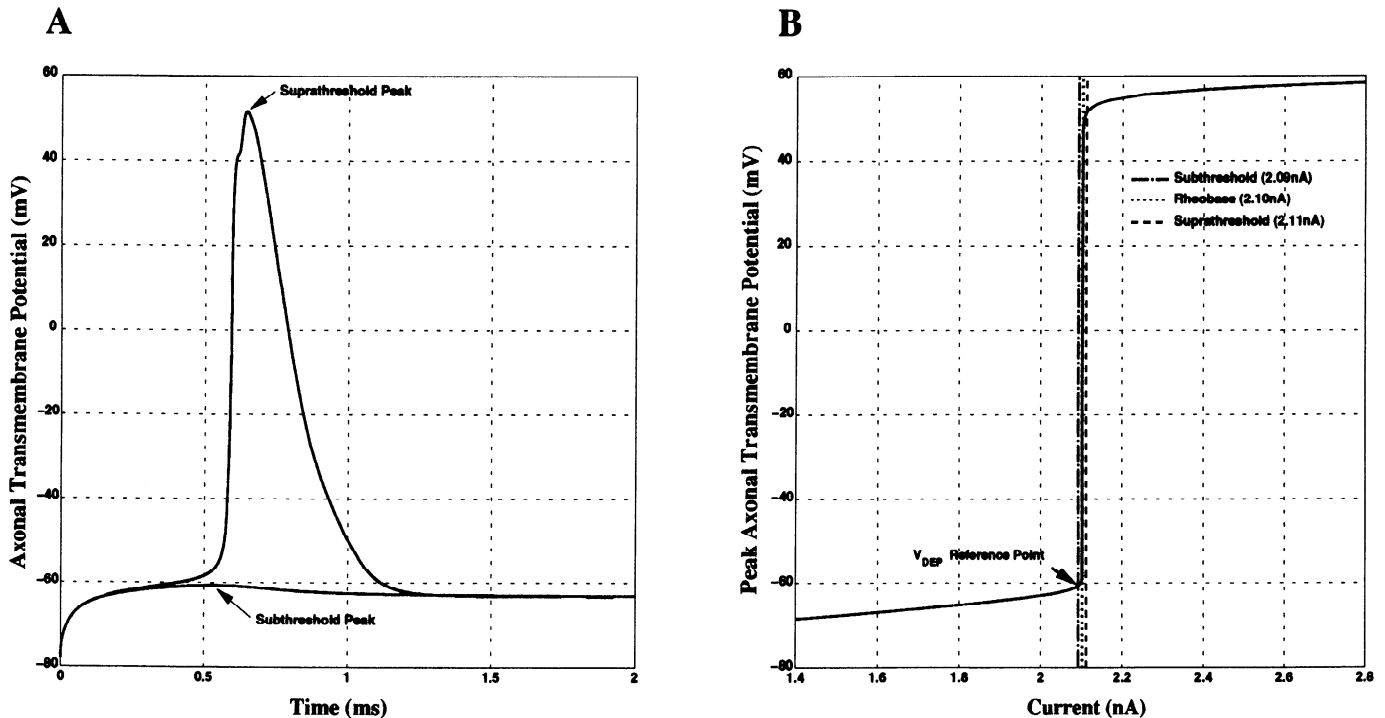


FIG. 1. A: axonal transmembrane potential for sub- and suprathreshold long-duration current pulses. B: peak axonal transmembrane potential vs. amplitude of the long-duration current pulses. Note the highly nonlinear character of this voltage-current relationship in the region near rheobase. Because of this nonlinearity, the subthreshold current (rheobase minus 10 pA) was used as a reference point for V_{DEP} .

permeability (---). It indicates that the experimentally observed reduction of 4.4 m/s in CV could be reproduced by a +2.2-mV shift in activation voltage or by a 22% reduction in permeability. Equivalent reductions in CV were obtained for each of the other parameters (see Table 3), although very large shifts were required in some parameters (e.g., a 131,945% increase in nodal K_{fast} was needed to reproduce the 4.4-m/s decrease in CV).

Values of V_{DEP} and APA were also calculated over comparable ranges of values for each parameter. Figure 2B shows the predicted dependence of V_{DEP} on the voltage dependence of Na⁺ channel activation voltage and on peak Na⁺ channel permeability. The +2.2-mV shift in activation voltage that produces the observed decrease in CV increases V_{DEP} by 2.6 mV, which is close to the observed 2.1-mV increase. In contrast, the 22% drop in permeability required to produce the observed decrease in CV increases V_{DEP} by only 0.8 mV. In addition, the +2.2-mV shift in Na⁺ channel activation voltage also reproduces the minimal change observed in APA, whereas the reduction in permeability predicts a substantial reduction in APA. Table 3 summarizes these results and also shows the effects on V_{DEP} and APA of other changes in active or passive properties or structure. Only the shift in Na⁺ channel activation voltage accounts for both the observed change in V_{DEP} and the minimal effect on APA.

DISCUSSION

The model's predictions as to the effects of changes in Na⁺ channel and other properties are consistent with other theoretical and experimental analyses (Hardy 1973; Moore et al. 1978; Sharp et al. 1993). They indicate that a positive

shift in Na⁺ channel activation voltage could account qualitatively and quantitatively for the experimental findings of lower CV, larger V_{DEP} , and slight decrease in APA. Thus they support the hypothesis that a positive shift in Na⁺ channel activation voltage is primarily responsible for operantly conditioned H-reflex decrease (Carp and Wolpaw 1994).

This hypothesis is largely consistent with the absence of significant change in other motoneuron properties measured, including resting membrane potential, input resistance, after-hyperpolarization, time constant, and electrotonic length. The only property measured by Carp and Wolpaw (1994) other than CV or V_{DEP} that would be expected to change with Na⁺ channel activation properties is rheobase (i.e., current threshold for eliciting a single action potential with a long-duration pulse). In addition to its dependence on Na⁺ channel properties, motoneuron rheobase probably depends on other active conductances [e.g., subthreshold calcium currents (Schwindt and Crill 1980, 1982)] that are not known to be present in the axon. The high degree of variability in rheobase measurements [i.e., SD was >50% of the mean (Carp and Wolpaw 1994)] is consistent with dependence on multiple mechanisms. Thus the rheobase predicted by this myelinated axon model is unlikely to be directly comparable with motoneuron rheobase.

CV, V_{DEP} , and APA reflect the integration of all properties of the myelinated nerve fiber. Thus multiple combinations of fiber parameters could produce similar behavior. This study begins from a point in the parameter space that is believed to be a good estimate of the properties of the healthy, intact large-diameter myelinated nerve fiber (Halter 1989). Although an exhaustive search of the parameter space might reveal other combinations of changes in parameters that could account for the experimental observations, the

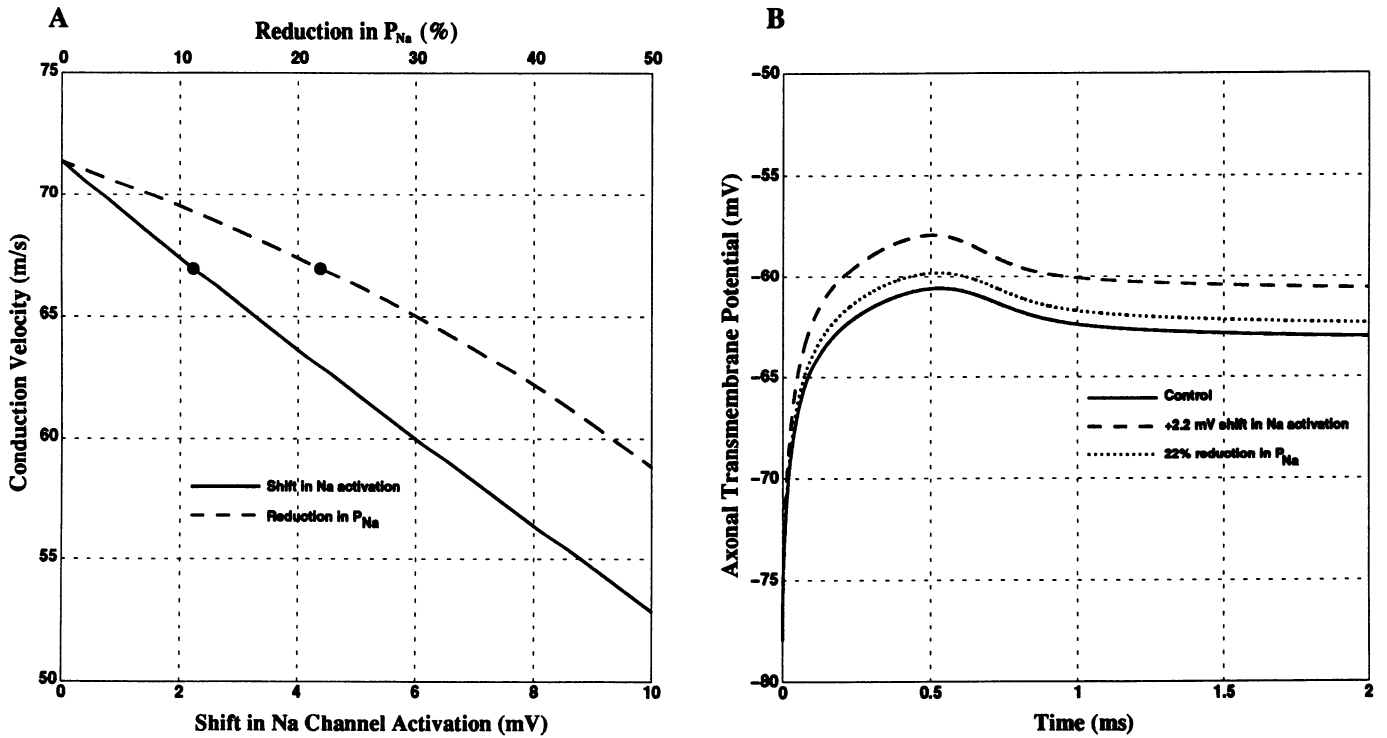


FIG. 2. A: predicted effects on conduction velocity (CV) of a 0- to 10-mV positive shift in Na^+ channel activation or a 0-50% reduction in Na^+ channel permeability. On each curve, a symbol indicates the change required to produce a CV reduction of 4.4 m/s, the value measured experimentally. B: predicted effects of these changes on the firing threshold. An intra-axonal constant current with an amplitude of 10 pA below rheobase was applied at a central node of Ranvier at *time* 0. A 22% reduction in Na^+ channel peak permeability produces a shift of +0.8 mV in peak axonal transmembrane potential. In contrast, a shift of +2.2 mV in Na^+ channel activation produces a shift of +2.6 mV in peak axonal transmembrane potential, which is close to the experimentally observed change of +2.1 mV in V_{DEP} (see text for full explanation).

physiological significance of such findings would be questionable. In the present analysis, the effects of varying single parameters were evaluated. Conditioning might change multiple neuronal properties. However, an exhaustive analysis of all possible combinations of model parameters is not warranted here because it is not clear which combinations are biologically relevant. Prompted by the observations of Numann (1991), we did explore the consequences of reduction in peak Na^+ permeability combined with increase in Na^+ channel inactivation time constant. Various combinations of these two parameters that reproduced the observed decrease in CV did not reproduce the observed values of V_{DEP} and APA.

The distributed-parameter myelinated axon model employed here is a robust tool for examining the functional implications of uniform and nonuniform changes in the anatomic and biophysical properties of the nerve fiber. However, it does not include an explicit representation of the properties of the axon hillock, dendrites, or soma. If nonuniform changes in the properties of these neuronal structures were hypothesized to be responsible for the experimental observations, a compartmental model of the whole motoneuron would be needed to examine the functional implications of these changes. However, the applicability of the myelinated axon model to estimates of V_{DEP} is supported by recent work indicating that neuronal spike initiation occurs in the initial segment of the axon (Huguenard et al. 1994).

The present analysis assumes that the experimental observation (Carp and Wolpaw 1994) of an increase in antidromic spike latency indicated a uniform reduction in CV along the

entire motoneuron axon. Although this is perhaps the simplest explanation, it is not the only one. The experimental finding could have resulted from a nonuniform change in CV along the axon, or even from a delay in initial segment or somatic response to the arrival of the antidromic action potential (although examination of the intracellular recordings provided no support for this latter possibility). Measurements of CV for different segments of the axon will be needed to resolve this uncertainty.

The descending pathways by which exposure to the operant conditioning task might change the voltage dependence of Na^+ channels are yet to be defined. However, recent studies suggest that the intracellular events triggered by these pathways may be mediated by protein kinase C (PKC). Meiri and Gross (1989) found that a phorbol ester that activated PKC increased the firing threshold and reduced the conduction velocity in rat sciatic myelinated nerve fibers. Similarly, Dascal and Lotan (1991) found that PKC activation caused a positive shift in the voltage dependence of Na^+ channel activation in rat and chick Na^+ channels expressed in *Xenopus* oocytes. On the other hand, Zhang and Krnjevic (1987) found in cat spinal motoneurons that a phorbol ester or PKC increased APA, and Szenté et al. (1990) reported that PKC inhibition in cat neocortical neurons increased the current injection needed to fire the cell and decreased APA. Both these reports suggest that PKC activation might produce a negative shift in Na^+ voltage dependence. Thus the first two studies suggest that the increase in V_{DEP} and decrease in CV accompanying operantly conditioned decrease in the H reflex could be due to PKC activation,

TABLE 3. Observed and predicted changes in CV, V_{DEP}, and APA in conditioned motoneurons

		ΔCV, m/s	ΔV _{DEP} , mV	ΔAPA, mV
Observed				
		-4.4	+2.1	-0.5
Predicted				
Parameter Changed	Amount of Change			
1) Na ⁺ channel activation voltage	+2.2 mV	-4.4	+2.6	-0.9
2) Na ⁺ channel activation time constant	+12%	-4.4	-0.1	-1.1
3) Na ⁺ channel inactivation voltage	-24.6 mV	-4.4	+1.4	-14.0
4) Na ⁺ channel inactivation time constant	-55%	-4.4	+3.9	-5.5
5) Nodal Na ⁺ channel peak permeability	-22%	-4.4	+0.8	-4.9
6) Nodal K _{fast} ⁺ channel permeability	+131,945%	-4.4	+2.6	-17.1
7) Nodal K _{slow} ⁺ channel permeability	+4,044%	-4.4	+0.4	-4.7
8) Nodal axonal conductance	+35%	-4.4	+0.4	-3.7
9) Myelin capacitance	+12%	-4.4	0.0	-1.0
10) Number of myelin lamellae	-11%	-4.4	+0.1	-1.1
11) Fiber diameter	-5%	-4.4	-0.1	-0.8
12) Periaxonal space width	+174%	-4.4	+0.2	-1.8

CV, conduction velocity; V_{DEP}, depolarization required to reach firing threshold; APA, action-potential amplitude.

whereas the latter two suggest that they could be due to PKC inactivation. In apparent contrast to all four studies, Numann et al. (1991), working with primary cultures of rat brain neurons and Na⁺ channels expressed in hamster ovary cells, found that PKC reduced P_{Na} and slowed inactivation without affecting the voltage dependence of activation/inactivation.

In sum, although its effects appear to vary across species, neuronal populations, and/or experimental preparations, PKC is a strong candidate for involvement in the changes in motoneuron threshold and CV found in operantly conditioned animals. Persistent activation of PKC is associated with long-term potentiation in hippocampal neurons (Klann et al. 1993). Whether PKC alters Na⁺ channel properties during normal CNS function in general, or during operant conditioning of the H reflex in particular, remains to be determined.

This work was supported by the Whitaker Foundation, Vivian L. Smith Foundation for Restorative Neurology to J. A. Halter, Paralyzed Veterans of America Spinal Cord Research Foundation to J. S. Carp, and National Institute of Neurological Disorders and Stroke Grant NS-22189 to J. R. Wolpaw.

Address for reprint requests: J. A. Halter, Div. of Restorative Neurology and Human Neurobiology, Baylor College of Medicine, One Baylor Plaza, Rm S809, Houston, TX 77030.

Received 3 October 1994; accepted in final form 27 October 1994.

REFERENCES

BERTHOLD, C.-H. AND RYDMARK, M. Anatomy of the paranode-node-paranode in the cat. *Experientia* 39: 964–976, 1983.

- CARP, J. S. Physiological properties of primate lumbar motoneurons. *J. Neurophysiol.* 68: 1121–1131, 1992.
- CARP, J. S. AND WOLPAW, J. R. Motoneuron plasticity underlying operantly conditioned decrease in primate H-reflex. *J. Neurophysiol.* 72: 431–442, 1994.
- DASCAL, N. AND LOTAN, I. Activation of protein kinase C alters voltage dependence of a Na⁺ channel. *Neuron* 6: 165–175, 1991.
- GERSHON, E., WEIGHL, L., LOTAN, I., SCHREIBMAYER, W., AND DASCAL, N. Protein kinase A reduces voltage-dependent Na⁺ current in *Xenopus* oocytes. *J. Neurosci.* 12: 3743–3752, 1992.
- HALTER, J. A. *A Distributed-Parameter Model of the Myelinated Nerve Fiber* (PhD thesis). Houston, TX: Rice Univ., 1989.
- HALTER, J. A., CARP, J. S., AND WOLPAW, J. R. Alteration in firing threshold and axonal conduction velocity of primate spinal motoneurons by H-reflex conditioning: theoretical analysis. *Soc. Neurosci. Abstr.* 19: 537, 1993.
- HALTER, J. A., CARP, J. S., AND WOLPAW, J. R. Do axons learn? Possible role of sodium channels in operantly conditioned motoneuron plasticity. *Soc. Neurosci. Abstr.* 20: 788, 1994.
- HALTER, J. A. AND CLARK, J. W., JR. A distributed-parameter model of the myelinated nerve fiber. *J. Theor. Biol.* 148: 345–382, 1991.
- HALTER, J. A. AND CLARK, J. W., JR. The influence of nodal constriction on conduction velocity in myelinated nerve fibers. *Neuroreport* 4: 89–93, 1993.
- HARDY, W. L. Propagation speed in myelinated nerve. II. Theoretical dependence on external Na⁺ and on temperature. *Biophys. J.* 13: 1071–1089, 1973.
- HUGUENARD, J. R., JOERGES, J., MAINEN, Z. F., AND SEJNOWSKI, T. J. Functional role of axon hillock and initial segment in cortical spike initiation. *Soc. Neurosci. Abstr.* 20: 1527, 1994.
- KANDEL, E. R. Cellular mechanisms of learning and the biological basis of individuality. In: *Principles of Neural Science*, edited by E. R. Kandel, J. H. Schwartz, and T. M. Jessell. New York: Elsevier, 1991, p. 1009–1031.
- KLANN, E., CHEN, S. J., AND SWEATT, J. D. Mechanism of protein kinase C activation during the induction and maintenance of long-term potentiation probed using a selective peptide substrate. *Proc. Natl. Acad. Sci. USA* 90: 8337–8341, 1993.
- MATSUMURA, M. AND WOODY, C. D. Long-term increases in excitability of facial motoneurons and other neurons in and near the facial nuclei after presentations of stimuli leading to acquisition of a Pavlovian conditioned facial movement. *Neurosci. Res.* 3: 568–589, 1986.
- MEIRI, H. AND GROSS, B. Modification of the Na-dependent action potential in myelinated fibers of rat sciatic nerve exposed to phorbol ester. *Brain Res.* 502: 401–409, 1989.
- MOORE, J. W., JOYNER, R. W., BRILL, M. H., WAXMAN, S. D., AND NAJER-JOA, M. Simulations of conduction in uniform myelinated nerve fibers: relative sensitivity to changes in nodal and internodal parameters. *Biophys. J.* 21: 147–160, 1978.
- NUMANN, R., CATTERALL, W. A., AND SCHEUER, T. Functional modulation of brain sodium channels by protein kinase C phosphorylation. *Science Wash. DC* 254: 115–118, 1991.
- SCHWARTZ, J. R. AND EIKHOF, G. Na currents and action potentials in rat myelinated nerve fibers at 20 and 37°C. *Pfluegers Arch.* 409: 569–577, 1987.
- SCHWINDT, P. C. AND CRILL, W. E. Properties of a persistent inward current in normal and TEA-injected motoneurons. *J. Neurophysiol.* 43: 1700–1724, 1980.
- SCHWINDT, P. C. AND CRILL, W. E. Factors influencing motoneuron rhythmic firing: results from a voltage-clamp study. *J. Neurophysiol.* 48: 875–890, 1982.
- SHARP, A. A., O'NEIL, M. B., ABBOTT, L. F., AND MARDER, E. Dynamic clamp: computer-generated conductances in real neurones. *J. Neurophysiol.* 69: 992–995, 1993.
- SZENTE, M. B., BARANYI, A., AND WOODY, C. D. Effects of protein kinase C inhibitor H-7 on membrane properties and synaptic responses of neocortical neurons of awake cats. *Brain Res.* 506: 281–286, 1990.
- WOLPAW, J. R. AND HERCHENRODER, P. A. Operant conditioning of H-reflex in freely moving monkeys. *J. Neurosci. Methods* 31: 145–152, 1990.
- ZHANG, L. AND KRNEVIC, K. Effects of intracellular injections of phorbol ester and protein kinase C on cat spinal motoneurons in vivo. *Neurosci. Lett.* 77: 287–292, 1987.